Numerical Simulation of a Two-Dimension Ramp Inlet Flow Field

Dr. Jalal M. Jalil* **&** **Ahmed F. Kridy***

Received:28/10/2008
Accepted:22/1/2009

Abstract

The Two-dimension ramp inlet flow field was studied with typical mode operations. Euler equations were used for solution with no special treatment required. In this work a solution algorithm based on finite difference MacCormack's technique was developed to solve mixed subsonic-supersonic flow problem through the external shock diffusers (ramp inlet) and it is found to be converge for supercritical and critical inlet operation.

Keywords: CFD, Supersonic, Ramp Inlet, Shock Capture, MacCormack's Technique.

التمثيل العددي لشكل الجريان ثنائي البعد في اخذة الهواء ذات السطح المنحدر

الخلاصة

تم في هذا البحث دراسة الجريان ثنائي البعد في اخذة هواء ذات السطح المنحدر لظروف عمل مثالية. استعملت معادلات اؤيلر للحل بدون معالجات خاصة. في هذا البحث تم تطوير اسلوب حل يعتمد على الفروقات المحددة وتكنيك ماكورمك لحل مسائل الجريان المختلط (تحت صوتي – فوق صـــوتي) خلال اخذة السطح المنحدر المصحوبة بالصدمة الخارجية و قد وجد ان الحل يقترب لظـــروف دخـــول حرجة وفوق حرجة

1. Introduction:

The problem of air intake design is to ensure that an aircraft engine is properly supplied with air under all conditions of aircraft operation and that the aptitude of the airframe is not unduly impaired in the process.

The computation of inlet flow field has been the subject of number of investigations. **Bangent, et al**, 1982[1], conducted an analytical study to determine the impact of flight Mach number on inlet type for a supersonic cruise aircraft. **Biringen**, 1984[2], outlines a time-implicit, finite-difference solution procedure for Euler equations, to calculate two-dimensional inlet flow fields. **Moretti**, 1988[3], presented an efficient Euler computational technique for two-dimensional Euler equation at any number of any shape and type, whose interaction can be treated by this technique. **Dimitri**, 1989[4], presented a simple theoretical method to determine the inviscid, steady state diffuser performance of a tunnel with two plane, parallel supersonic streams that come into constant downstream of a splitter plane and from an infinitely thin interface. **Singh Th. et al**. 2000[5], presented a study of the field of axi-symmetric, mixed-compression, supersonic air intakes for viscous flows. The governing equations of mass, momentum, energy, and state equation have been solved to obtain the complete flow field using the commercial software package (FLUENT). Recently CFD was used for supersonic inlet[6,7,8].

The present work mainly focuses on the calculation of inviscid inlet flow field with

*Electromechanical Engineering Department, University of Technology/Baghdad

uniform in flow boundary conditions; viscous effects, which can be important to simulate, flow reversal and separation are not considered.

The aim of the present work is to study numerically the two-dimension ramp inlet flow field for air breathing missiles in a two-shock system under the following conditions:

a. Free stream Mach number 1.6, 1.8, 2.0 and 2.2 in supercritical case at atmospheric conditions, pressure 101325 N/m^2 and temperature 15^{o}C.

b. The ramp angle (b) 4.67^o, 8.77^o, 10.62^o and 13.98^o at free stream Mach number 2.0.

c. Studying the operation of external shock diffusers (ramp inlet) in a critical case and supercritical case at Mach number 2.0.

2. Theoretical Analysis

The calculation of the inlet flow field is of considerable importance to the efficient design of air breathing missiles. These flow fields are very complex due to their mixed hyperbolic-elliptic nature, the influence for body and viscous effects, as well as three-dimensionality. The complexities of three-dimensional viscous inlet flow make their numerical prediction a very difficult task; therefore, the calculation of two dimensional inlets is an evolutionary step toward that direction. The ramp Inlet flow fields calculated by a two-dimensional computational method, the problem of employing an explicit, time-marching, finite difference procedure to solve the Euler equation formulated in body-fitted coordinates. The method can be used for a flow field in both supersonic and subsonic regions.

2.1. Algebraic Grid Generation Techniques:

The algebraic equation is used to relate the grid points in the computational domain to those of the physical domain. This objective is met by using an interpolation scheme between the specified boundary grid points to generate the interior grid points. Clearly, many algebraic equations can be introduced for this purpose. The physical domain is depicted in Figs. 1 and 2.

2.2. Governing equations

For high Reynolds number flows, viscous effects are confined to the vicinity of the surface, where large velocity gradients exist. This region is known as the boundary layer. Outside the boundary layer, the velocity gradients are negligible resulting in zero shear stresses. This region is called the inviscid region, and solution procedures for the inviscid flow region are governed by the Euler equations and the present solution is depends upon this approach, in which it is written in conservation-law form for two-dimensional flows of a perfect gas[9,10,11].

The general compact vector form is given as:-

$$\frac{\partial U}{\partial t}+\frac{\partial E}{\partial x}+\frac{\partial F}{\partial y}=0$$

where :

$$U=\begin{bmatrix} r \\ ru \\ rv \\ re_t \end{bmatrix} \quad , \quad E=\begin{bmatrix} ru \\ ru^2+p \\ ruv \\ u(e_t+p) \end{bmatrix} \quad , \quad F=\begin{bmatrix} rn \\ run \\ rn^2+p \\ n(e_t+p) \end{bmatrix} \qquad \ldots. (1)$$

u and v are the velocities along the x and y coordinates, respectively, p is the pressure, r is the density, and e_t is the total energy per unit volume. And U, E, F are the fluxes vectors.

To transform the Euler Equation (1) into curvilinear coordinates (x,h), an independent variable may be written as follows:-

$$\frac{\partial \bar{U}}{\partial t}=-\frac{\partial \bar{E}}{\partial x}-\frac{\partial \bar{F}}{\partial h}$$

Where:

$$\bar{U}=U/J, \bar{E}=\frac{Ex_x+Fx_y}{J} \ , \ \bar{F}=\frac{Eh_x+Fh_y}{J}$$

2.3. Time Step Calculation:

The value of Dt cannot be arbitrary, rather it must be less than some maximum values for stability, it was stated that Dt must obey the Courant-Friedriches-Lowry criterion CFL. The CFL criterion states that physically the explicit time step must be not greater than the time required for a sound wave to propagate from one grid to next. The maximum allowable value of CFL factor for stability in explicitly time dependent finite difference calculation can

vary from approximately 0.5 to 0.1. To determine the value of time step, the following version of the *CFL* criterion [12] is used. Where $a_{i,j}$ is the local speed of sound in meters per second, and *C* is the coefficient.

$$(\Delta t_{CFL})_{i,j} = \left[\left| \frac{u_{i,j}}{\Delta \xi} \right| + \left| \frac{v_{i,j}}{\Delta \eta} \right| + a_{i,j} \sqrt{\frac{1}{\Delta \xi^2} + \frac{1}{\Delta \eta^2}} \right]^{-1} \quad \ldots (2)$$

and , $Dt = min\ [C\ (Dt_{CFL})_{i,j}]$.

2.4. Boundary Condition:

The Euler equation has an unlimited number of solutions. What makes a solution unique is the proper specification of initial and boundary conditions for a given *PDE* (Euler equation). A set of boundary conditions must be specified, it referred to as the "analytical boundary condition" Once the *PDE* is approximated by a *FDE*, Thus the *FDE* will require additional boundary conditions. This boundary condition will be referred to as "numerical boundary condition". As for the problem under consideration, there are four types of boundaries: solid, inflow, outer and outflow.

For the three solid boundary conditions (ramp, inside and outside cowl), the tangency grid body surface must be satisfied for inviscid flow. The components of the momentum equation for the two-dimension flow may be expressed with some mathematical steps [13], as:-

$$\left.\begin{aligned} &\eta_x\left(\frac{\rho u \bar{U}}{J}\right)_\xi + \eta_y\left(\frac{\rho u \bar{U}}{J}\right)_\xi + \eta_x\left(\frac{\rho v \bar{V}}{J}\right)_\eta + \eta_x\left(\frac{\rho u \bar{V}}{J}\right)_\eta \\ &+ \eta_x\left(\frac{\xi_x p}{J}\right)_\xi + \eta_x\left(\frac{\eta_x P}{J}\right)_\eta + \eta_y\left(\frac{\xi_y P}{J}\right)_\xi + \eta_y\left(\frac{\eta_y P}{J}\right)_\eta = 0 \end{aligned}\right\} \quad \ldots (3)$$

a. Ramp surface & upper cowl surface:
A finite difference equation for the upper equation is obtained, as a second order central difference approximation for the *x* derivatives and a second order forward difference approximation for *h* derivatives are used.

b. Lower cowl surface:
A second order central difference approximation for *x* derivatives and second-order backward difference approximation for *h* derivatives are used.

The outer flow boundary the air flow out from the numerical simulation of two-dimensional ramp inlet at 1.4 meter far from the original point *O*. To calculate the properties at this boundary first order backward transformation derivatives are used (smooth exit).

The outflow boundary illustrated in Fig. 1 represents air flow out from the numerical simulation of two-dimension ramp inlet 2.0 meter far from the original point *O* above the inlet duct and the airflow out from the ramp inlet duct.

a. Using background derivatives to obtain the air flow properties above the inlet.

b. For **completely supercritical** case (supersonic outflow boundary) the back ward transformation derivatives are used.
.

c. For **critical and supercritical** cases (subsonic outflow boundary) the back pressure at the duct outflow boundary P_o was set to a value high enough to ensure subsonic outflow boundary and the other properties are obtained from the background transformation derivatives.

3. Result and Discussions:

The intake characteristics of the supersonic aircraft are dominated by the shock-wave systems that go into their design. In the following results temporarily the problems of boundary layer and flow separation not taken into consideration and consider the simple nature and properties of shock system. The simplest form of staged compression is the two shock intake in which a single wedge project is formed of the duct. To survey the fundamental parameters affecting the shock system, the next subsections will give some details.

Figure 3, *a* presents the two-dimension ramp inlet with *1.6* Mach number as inflow using a grid with *60* nodes along *x* and *120* nodes along *h* direction. Results are obtained from calculations with supersonic out flow boundary conditions. In this case the flow is completely supersonic, the figure shows

the details of Mach number contour. The initial oblique ramp shock and the shock at the cowl lip are clearly depicted. The internal oblique shock waves are followed by a change of ramp shape at point *B* and *c*, occurring at some shock smearing due to the calculation procedure. The ramp angle is 9^o and the ramp position is *23 cm* far from the original point *O*. At cowl lip, the normal shock occurs outside the inlet, while the flow inside the inlet increases by the influence of the divergent shape. The initial oblique shock is 49.5^o measured from *x*-axis. Figure 3, *b* with *1.8* Mach number as in flow boundary. The initial oblique shock is 42.8^o measured from *x*-axis. Figure 3, *c* presents the two-dimension ramp inlet with *2.0* Mach number, with 60×120 grids and for the same ramp angle and ramp position, the calculations are performed with supercritical outflow boundary condition (completely supersonic). Figure 3, *d* presents Mach contour resulting from *2.2* in-flow Mach number with the same condition of upper figures.

Figure 4 (*a, b, c* and *d*) presents the two-dimension ramp inlet with *2.0* Mach number and 60×120 grids. The ramp is *27cm* far from the original point. Results are obtained from program calculation with supercritical out flow boundary (completely supersonic).

To study the properties of ramp inlet operation external shock diffuser, the typical modes of inlet operation are (critical and supercritical case). Thus Figure 5, *a* represents Mach contour in the critical case of ramp inlet operation, inflow Mach number is *2.0*. The ramp angle is 11.75^o and the ramp is *33.8cm* far from the original point *O*. The initial oblique shock is 41^o as illustrated in figure. Figure 5, *b* shows the pressure contour. Figure 5, *c* illustrates the temperature contour. Figure 5, *d* illustrates the pressure recovery results from calculation in critical case (P_{inline}/ P_{inflow}).
The supercritical operation occurs at the same mass flow as critical operation, but with increased losses, since the normal shock occurs at a higher Mach number and inside the inlet duct as illustrated bellow: The supercritical operation occurs at the same mass flow as critical operation, but with increased losses, since the normal shock occurs at a higher Mach number and inside the inlet duct. Figure 6, *a* illustrates Mach contours. Figure 6, *b* illustrates the pressure contour result from the supercritical case at Mach *2.0*. Figure 6, *c* illustrates the temperature contour. Figure 6, *d* illustrates the pressure recovery along ramp inlet center line. For the upper modes of ramp inlet operation the pressure was calculated along the center line passing through the ramp inlet duct. The total pressure, Fig. 5-*c* and Fig. 6-*c* illustrate the drop in total pressure in the two inlet mode operation.

4. Conclusions:

1. The implementation of MacCormack's scheme succeeded in predicting the mixed subsonic-supersonic flow domain.
2. The conservation form of partial differential equations has succeeded in predicting the location, strength of the shock wave.
3. There is no solution that can be obtained for shock capturing without the addition of artificial viscosity to the partial differential equation.
4. The value of 0.1 for **C**ourant-**F**reedrichs-**L**ewy (CFL) factor is used successfully for solving explicit Euler equations.
5. Body fitted coordinates have succeeded in the prediction of flow characteristic through the complex boundary.

5. Recommendations:

1. Extending the work to three-dimensional flow with shock capturing.
2. Extending the work with partial different grid generation methods.
3. Extending the work to include different shapes of ramp inlet to improve the recovery.
4. Extending the work to three shock system ramp inlet with two ramp angle.

References:

[1] Bangent, L.H., Santman, D.M., and Miller, L.D., "Some Effects of cruise speed and Engine Matching on Supersonic Inlet Design", Aircraft Journal, Vol.19, No.1, Jan. 1982.

[2] Biringen S., Numerical Simulation of Two-Dimension Inlet Flow fluid", Aircraft Journal, Vol.21, No.4 p.p. 212-215, April 1984.

[3]Moretti, and Gino, "Efficient Euler Solver with Many applications" AIAA Journal, Vol. 26, No.6, p.p. 755-757, June 1988.

[4]Dimitri P., Diffuser Performance of Two-Stream Supersonic Wind Tunnels", AIAA Journal Vol.27, No.8, Aug. 1989.

[5]Sigh Th. R., Chandran B.S.S., Belou V., and Sundaraagan, T., "Numerical Simulation of Supersonic Mixed Compression Axi-symmetric Air Intakes", NCABE, Dec.2000.

[6]Slater, J.W. "CFD methods for computing the performance of supersonic inlets" AIAA-2004-3404, July 2004.

[7]Slater, J.W., Davis, D.O., Sanders, B.W. and Wier, L.G. "Role of CFD in aerodynamic and analysis of the parametric inlet" AIAA, ISABE-2005-1168, 2005.

[8]Anderson B.H., Gibb J. "Application of CFD to the study of flow control for the management of inlet distortion" AIAA paper 92-3177, 1992.

[9]Raymer, D.P. "Aircraft Design : A conceptual Approach", 2nd Edition AIAA Education Series, Washington 1992.

[10]Hill, P.G. and Peterson, C. R., "Mechanics and Thermodynamics of Propulsion", Addison-Wesley Publishing Co., New Jersey, 1970.

[11]Seddon, J. and Goldswith, E. L., Intake Aerodynamics", Collins Professional and Technical Books, William Collins & Co. Ltd. London, 1985.

[12] JOHN. D. ANDERSON, TR., "Computational Fluid Dynamics", Department of Aerospace Engineering University of Maryland, McGraw-Hill, New York, International Editions 1995.

[13]KLAUS A. HOFFMANN, "Computational Fluid Dynamics for Engineers". The University of Texas at Austin, A Publication of Engineering Education System ™, Austin, Texas 78713, USA 1989.

Table 1, Initial oblique shock wave angles with different inflow Mach number.

The figure	Mach number	Ramp angle (b^o)	Initial oblique shock angle	
			Numerical solution (deg.)	Exact solution (deg.)
Fig. 3,*a*	1.6	9	49.5	49.52
Fig. 3,*b*	1.8	9	42.8	42.83
Fig. 3,*c*	2.0	9	38.2	38.24
Fig. 3,*d*	2.2	9	34.0	34.08

Table 2, Initial oblique shock wave angles with different ramp angles

The figure	Mach number	Ramp angle (β^o)	Initial oblique shock angle	
			Numerical solution (deg.)	Exact solution (deg.)
Fig. 4,a	2.0	4.67	34.0	34.0
Fig. 4,b	2.0	8.77	38.0	38.0
Fig. 4,c	2.0	10.62	40.0	40.0
Fig. 4,d	2.0	13.98	44.0	44.0

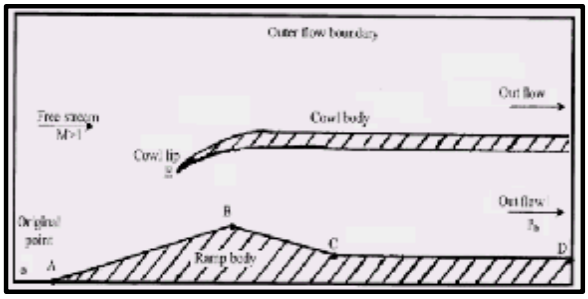

Figure (1) Two dimension ramp inlet (general shape)

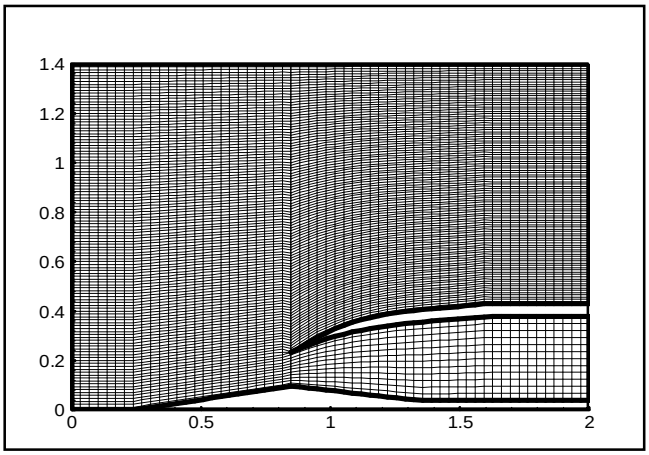

Figure (2) Two dimensional ramp inlet with 60*100 grid

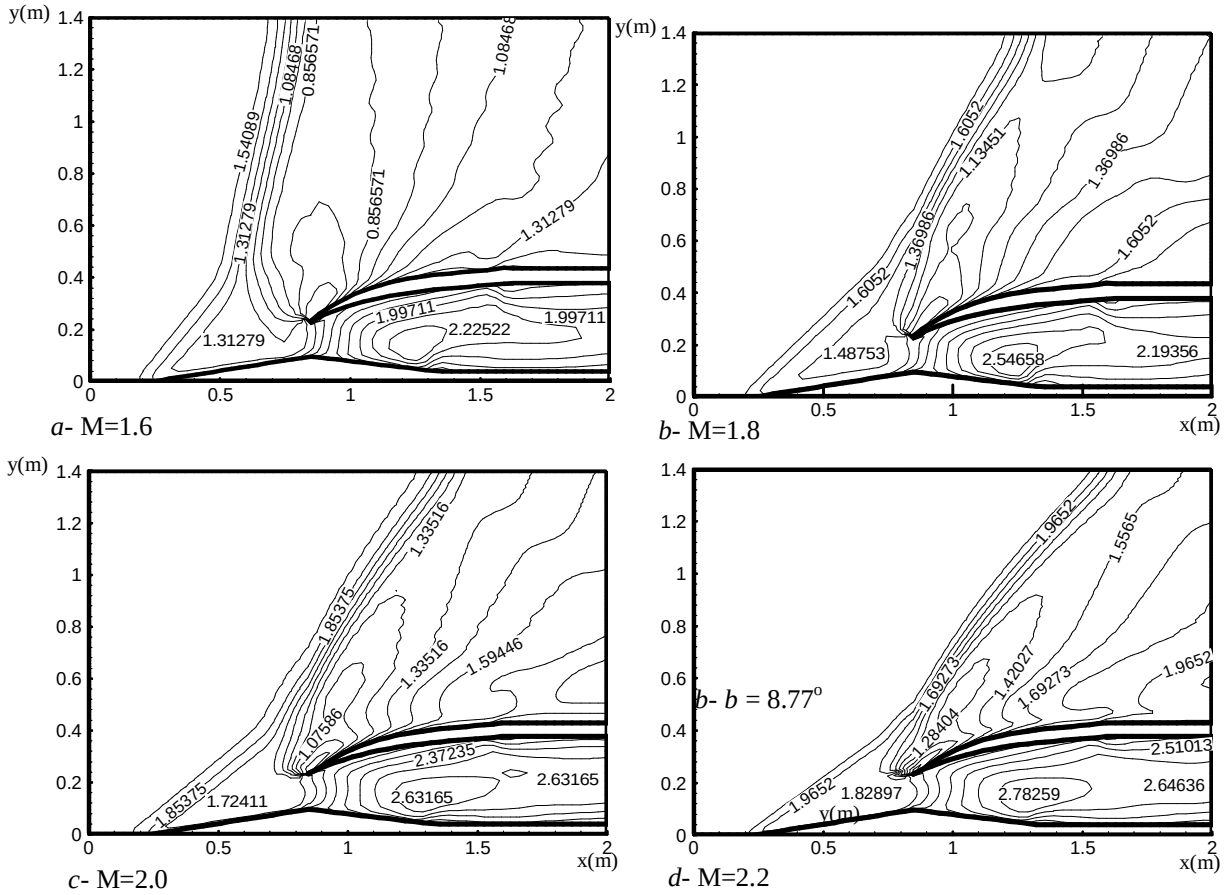

Figure (3) Mach contour, supercritical case with 60x120 grids, ramp angle *b* = *9°* and ramp body *23cm* from the original point for deferent free stream Mach number.

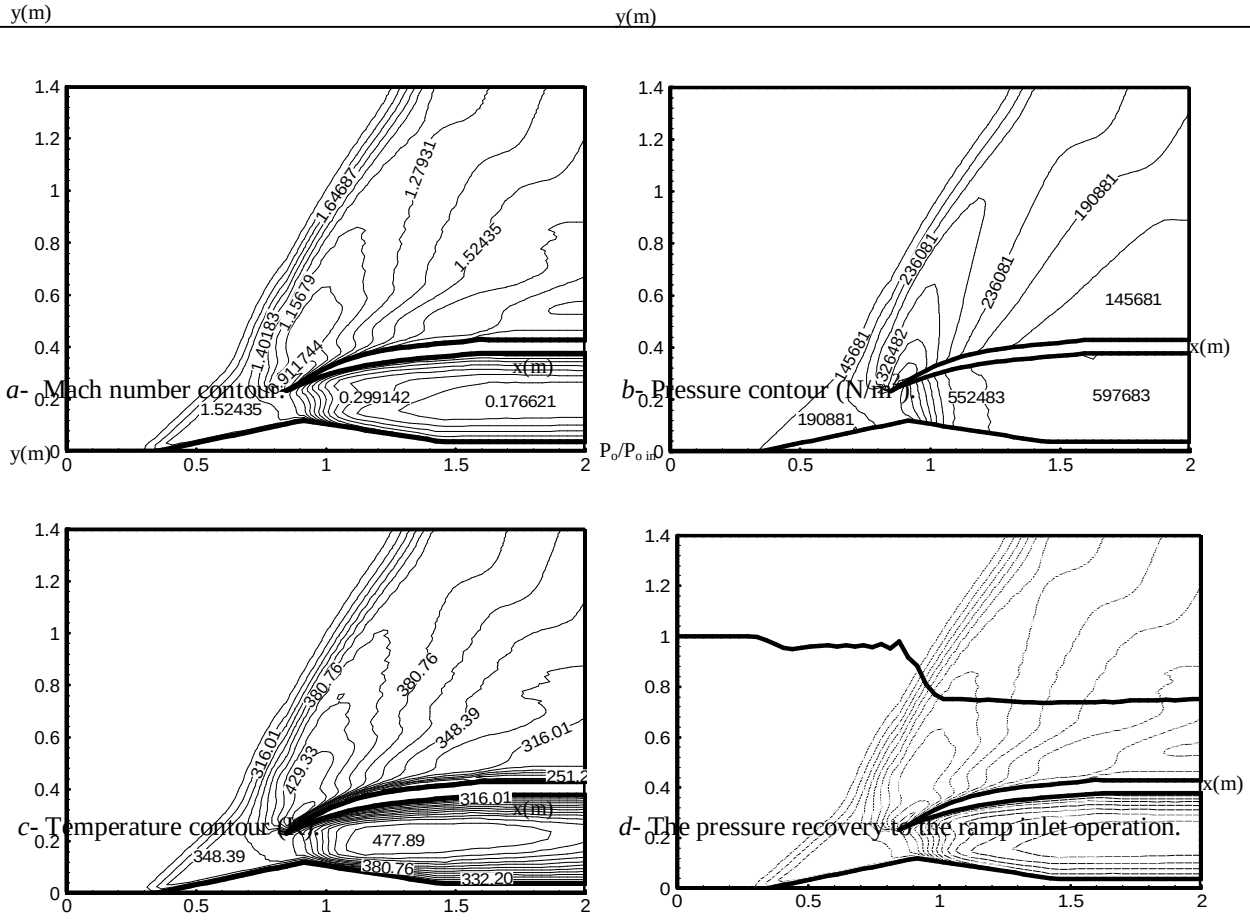

a- Mach number contour. *b*- Pressure contour (N/m²).

c- Temperature contour (K). *d*- The pressure recovery to the ramp inlet operation.

Fig. 5 Variation of properties of critical case (P_b= 0.75*$P_{o\ inflow}$) with 60*120 grids free stream Mach number 2.0, ramp angle 11.75°, ramp position 33.8*cm* far from original point .

original point for deferent ramp angle.